



ELSEVIER

Available online at [www.sciencedirect.com](http://www.sciencedirect.com)

SCIENCE @ DIRECT®

Journal of Magnetism and Magnetic Materials 294 (2005) 239–244

**M** Journal of  
**M** magnetism  
**M** and  
**M** magnetic  
materials

[www.elsevier.com/locate/jmmm](http://www.elsevier.com/locate/jmmm)

# Characterization of soft ferromagnetic materials by inductance spectroscopy and magnetoimpedance

R. Valenzuela\*, H. Montiel, M.P. Gutiérrez, I. Betancourt

*Instituto de Investigaciones en Materiales, Universidad Nacional Autónoma de México, P.O. Box 70-360, 04510 Mexico*

Available online 21 April 2005

---

## Abstract

Inductance spectroscopy and magnetoimpedance are extremely sensitive to a wide variety of intrinsic and extrinsic magnetic properties of soft magnetic materials; as a result, they can be used as a characterization tool. In this paper, the basic principles underpinning these magnetic phenomena are briefly discussed. The use of equivalent circuits is presented, as well as the correlations between the elements of such circuits and the relevant physical parameters of materials. Some specific cases are discussed.

© 2005 Elsevier B.V. All rights reserved.

*PACS:* 75:70.i; 75:50.Kj; 75:90.+d

*Keywords:* Inductance; Magnetoimpedance; Domain wall relaxation and resonance

---

## 1. Introduction

Inductance spectroscopy (IS), i.e. the measurement of complex inductance as a function of the frequency of the excitation magnetic field, is becoming an important methodology to characterize ferro- and ferrimagnetic materials [1–3]. Since complex magnetic permeability is proportional to complex inductance,  $\mu^* = KL^*$  (with  $K$  = geometrical constant), inductance measure-

ments are virtually equivalent to permeability measurements. These analyses are based on the fact that all magnetization processes contribute to the total magnetization, but they can be resolved by measuring at different frequencies because they possess different dynamics, or different time-constants. The value of permeability in each frequency range, the frequency at which a process becomes unable to follow the excitation field, and also the dispersion (the manner a magnetization process changes from a process to another one) are significant and contribute to the understanding of dynamical magnetization phenomena.

Magnetoimpedance (MI) refers to the variations in the impedance response of a ferromagnetic

---

\*Corresponding author. Tel.: +52 55 5622 4653;  
fax: +52 55 5616 1371.

*E-mail address:* [monjaras@servidor.unam.mx](mailto:monjaras@servidor.unam.mx)  
(R. Valenzuela).

conductor (subjected to a high-frequency electric current of low amplitude), when a DC magnetic field is applied. Although first described several decades ago [4], it has recently raised interest because of its technological applications in the sensor field [5]. The physics involved in MI (domain wall magnetization processes at low frequency, skin depth effects and spin rotations at high frequencies) are also of basic interest [6]. A variety of factors modulate MI: induced anisotropies [7], AC current amplitude [8], domain structure [9], magnetostriction [10], applied stresses [11,12], helical anisotropies [13–15], etc. Both methods, IS and MI, can be combined as a tool to investigate the intrinsic and extrinsic properties of magnetic materials, as presented in this paper.

## 2. Domain wall dispersion

The basic magnetization processes, spin rotation, domain wall bulging and domain wall displacement, possess different dynamics; they respond to excitation fields up to a given frequency. They have different time-constants. As a consequence, they can be resolved by means of measurements at different field frequencies. Since spin rotation is the most simple process, it shows a dispersion at the highest frequencies (ferromagnetic resonance), in the gigahertz range. Domain wall bulging involves the collective movement of the spins within a wall, and exhibits a dispersion at lower frequencies than spin rotation, typically in tens to hundreds of kilohertz for metals [16]. In the case of domain wall displacements, the amount of spins that are collectively inverted is much higher, and therefore this process is associated with a low dispersion frequency.

In this paper, we focus on the domain wall bulging process and its dispersion. It is assumed that such a process occurs when the domain wall is pinned (to any defect such as grain boundaries, precipitates, pores, the external surface of the sample, other domain walls, etc.), and is bulged by the “pressure” of the applied field. The dispersion frequency and the dispersion itself are very significant. A basic way to study this dispersion

is the equation of motion,

$$m d^2x/dt^2 + \beta dx/dt + \alpha x = 2M_s H(t), \quad (1)$$

where  $m$  is the domain wall effective mass,  $x$  is the bulging,  $t$  is the time,  $\beta$  is the damping factor,  $\alpha$  is the spring constant,  $M_s$  is the saturation magnetization and  $H(t)$  is the excitation field. This is a very general equation which can be applied to a wide variety of physical phenomena. For a periodic excitation field,  $H(t) = H_0 \exp[-j\omega t]$ , where  $H_0$  is the field amplitude,  $j$  the basis of imaginary numbers and  $\omega$  is the angular frequency, Eq. (1) can be solved as follows:

$$x = A \exp(-j[\omega t - \phi]), \quad (2)$$

where  $A$  is a constant and  $\phi$  is a phase difference. This process has a characteristic frequency,  $\omega_R = [\alpha/m]^{1/2}$ , which is clearly a resonance frequency. To our knowledge, however, all ferromagnetic metals show a domain wall permeability dispersion which is different from a resonance process, as shown in Fig. 1. This dispersion is much closer to a relaxation process, characterized by a decrease in real permeability,  $\mu'$ , a maximum in imaginary permeability,  $\mu''$ , and a semicircle in the Cole–Cole representation (in inset). A natural resonance process, in contrast, exhibits a strong increase in the real part just before the resonance frequency, followed by a vertical decrease through

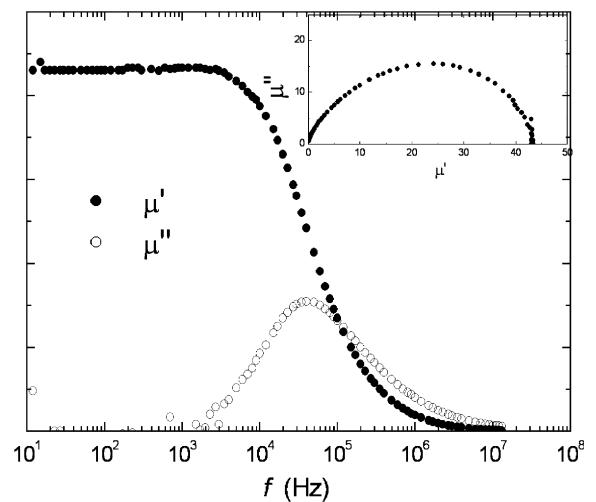


Fig. 1. Real and imaginary parts of permeability of a CoFeBSi amorphous ribbon [17].

the frequency axis toward negative values, and finally, an asymptotic approximation to zero. The imaginary part shows a strong maximum, and the Cole–Cole plot is a full circle.

In order to explore the effects of the several parameters on the response of the system, we derived expressions for its mechanical impedance,

$$Z' = \frac{[\omega(1/\alpha)(1 - \omega^2(m/\alpha) - \omega(m/\beta^2))]}{\{[1 - \omega^2(m/\alpha)]^2 + (\omega m/\beta)^2\}}, \quad (3)$$

$$Z'' = (1/\beta)/\{[1 - \omega^2(m/\alpha)]^2 + (\omega m/\beta)^2\}, \quad (4)$$

where  $Z'$  and  $Z''$  are the real and imaginary parts of mechanical impedance, respectively. From these expressions, we can obtain the relative effects of the  $m, \alpha$  and  $\beta$  parameters. It appears that the strongest effects depend on the  $\beta/m$  ratio. In fact, for  $\beta \ll m$ , i.e. when inertia dominates damping, the dispersion is effectively a resonance phenomenon. As the damping factor increases as compared with the effective mass, the dispersion changes toward a mixed behavior, and for  $\beta$  values very large, the dispersion becomes a relaxation. If the inertia term is neglected in Eq. (1), we have (Figs. 2 and 3)

$$\beta dx/dt + \alpha x = 2M_s H(t), \quad (5)$$

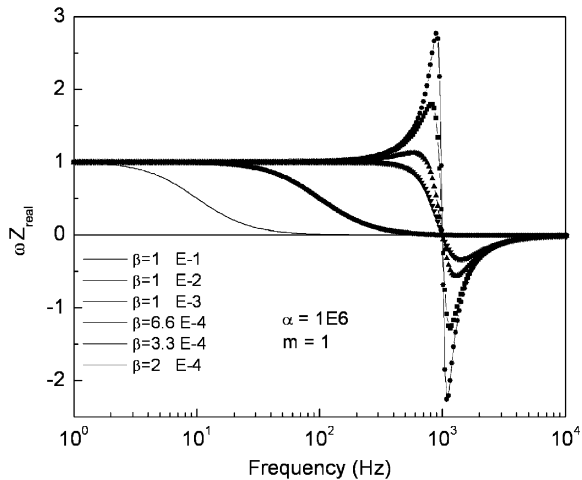


Fig. 2. Real part of mechanical impedance, as derived from Eq. (4), for several values of  $\beta$ , while  $\alpha$  and  $m$  are kept constant at 1 E6 and 1, respectively.

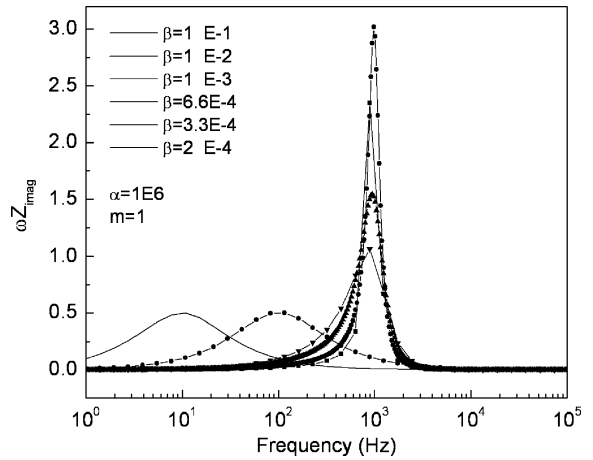


Fig. 3. Imaginary part of the mechanical impedance, as in Fig. 2.

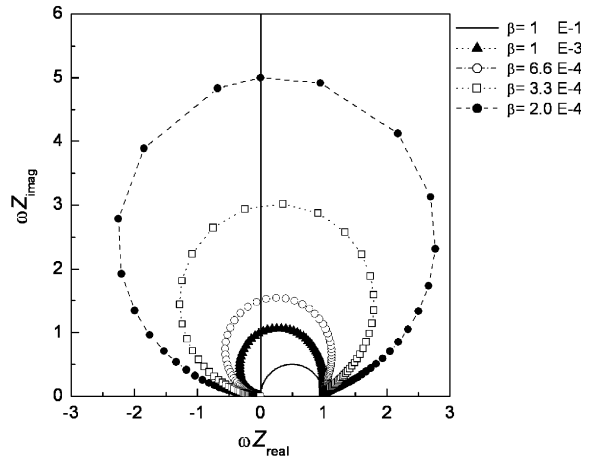


Fig. 4. Cole–Cole plot for several values of  $\beta$ , as in Fig. 2.

which leads to a relaxation frequency  $\omega_X = \alpha/\beta$ . The locus of relaxation in a Cole–Cole plot is effectively a semicircle. At this point, it is interesting to note that the ideal relaxation process leads to a perfect semicircle (Fig. 4), while typical experimental results are associated with a deformed semicircle. An explanation can be given in terms of the time-constant of the dispersion [18]: while the simple calculation from Eq. (6) is based on a single time-constant, it would be needed to consider a distribution of time-constant for the experimental results, since there are a collection of

pinned domain walls with a distribution in their free-bulging area, which is the magnetization process associated with this dispersion.

In contrast to metals, many experimental results obtained [19] on ferrimagnetic oxides (ferrites) show a dispersion closer to a resonance than to a relaxation. Since metals possess a much higher conductivity (typically 6 orders of magnitude), domain wall bulging produce local changes in magnetic flux, and this leads to the generation of local eddy currents (as a consequence of the Faraday's induction law). This additional process (as compared with oxides) can be expected to contribute to the total damping factor;  $\beta$  is larger in metals than in ferrites, and therefore the former will show a relaxation dispersion.

IS has been used to study the nanocrystallization process from an amorphous precursor [20]. In addition to a strong increase in the real part of permeability, the relaxation frequency shows a decrease that is close to a relationship of the form  $\mu f_X = \text{constant}$ .

### 3. Equivalent circuits

An interesting approach to the impedance response in ferro- and ferrimagnetic materials is provided by the use of equivalent circuits. In this methodology [2], the behavior of the material is modeled by means of an equivalent circuit. With the modern computing facilities, it is always possible to find a circuit which can represent virtually any experimental results. The best approach is then to explore first the simplest circuits, and then, to look for a clear correlation between the elements of the circuit and the physical parameters of the sample. By following this procedure, it is now clear that the simplest representation of relaxation is a RL parallel circuit. Of course, this simple modeling assumes a single time-constant. The relaxation frequency is  $\omega_X = R/L$ .

The case of a resonant dispersion can be modeled by means of a RCL circuit. A proposed [21] arrangement of the equivalent circuit elements is a RL series arm, in parallel with a capacitor C. The resonance frequency becomes of course

$\omega_R = (1/LC)^{1/2}$ . By considering the case of a domain wall pinned along two parallel edges with a cylindrical bulging, the DC magnetic permeability is [22]

$$\mu_0 = 8\pi M_s^2 d / 9\gamma, \quad (6)$$

where  $d$  is the distance between pinning edges and  $\gamma$  the domain wall energy. The spring constant is directly related to the domain wall energy as

$$\alpha = 18\gamma/d^2. \quad (7)$$

After some algebra, and taking into account a geometrical factor,  $K$ , to transform the complex inductance,  $L^*$ , into complex permeability,  $\mu^* = KL^*$ , it is possible to find a correlation between the equivalent circuit elements and the physical parameters in the equation of motion, for the relaxation dispersion, as follows:

$$\alpha = [16\pi M_s^2 / Kd](1/L), \quad (8)$$

$$\beta = [16\pi M_s^2 / Kd](1/R). \quad (9)$$

Wall mass can be related to the equivalent circuit capacitor as

$$m = [16\pi M_s^2 / Kd]C. \quad (10)$$

It appears that the equivalent inductor,  $L$ , is associated with the inverse of the spring constant; the amount of the bulging is proportional to the permeability value, and also inverse to the restoring force, which is a kind of wall rigidity. The damping factor, with its energy dissipation character, depends on the inverse of the equivalent resistor,  $R$ , which can be understood in terms of the relaxation frequency, Eq. (9), by considering the domain wall as a vibrating chord. A small damping (with a constant restoring force) leads to a high relaxation frequency. The effective domain wall mass is proportional to the equivalent capacity,  $C$ , which is consistent with the general idea that the inertia term depends on energy storing.

Since all the equivalent circuit elements can be extracted from experimental data (as far as these simple equivalent circuits provide an acceptable modeling), these correlations allow the direct evaluation of the microscopical parameters (Fig. 5).

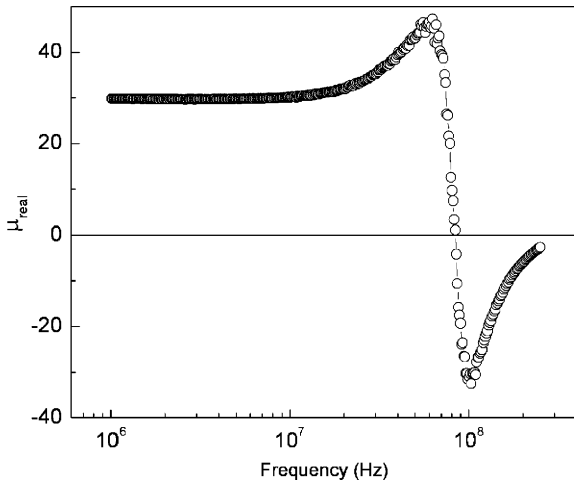


Fig. 5. Behavior of the real part of permeability in a  $\text{Ni}_{0.7}\text{Zn}_{0.3}\text{Fe}_2\text{O}_4$  ferrite [23].

#### 4. Magnetoimpedance

MI has become a powerful tool for characterization of soft ferromagnetic materials. In the typical arrangement, i.e., a wire (or microwire) or a ribbon with a circumferential or a transverse easy axis, respectively, and with the DC field applied parallel to the wire or ribbon axis, it is possible to evaluate the anisotropy field of the sample, as associated to the maxima appearing on  $\Delta Z/Z$  vs.  $H_{dc}$  plots. The existence of a helical anisotropy in as-cast amorphous wires has been recently investigated [13–15]. The effect of torsion is shown in Fig. 6 [15]. Since the separation between maxima is proportional to the anisotropy field, any factors affecting this field can be observed on the plot. Fig. 6 shows experimental results obtained on CoFeBSi wires (125  $\mu\text{m}$  diameter, 10 cm long), when a torsion stress is applied. The decrease in the two maxima separation as a function of stress, exhibits a counterbalancing of torsion stresses generated during fabrication of the wire. From these results, it was possible to calculate the magnetostriction factor [15].

MI has often been used to study the effects of thermal treatments. In an early study, the effects of aging, annealings and recovery in Metglas ribbons were investigated by frequency measurements [24].

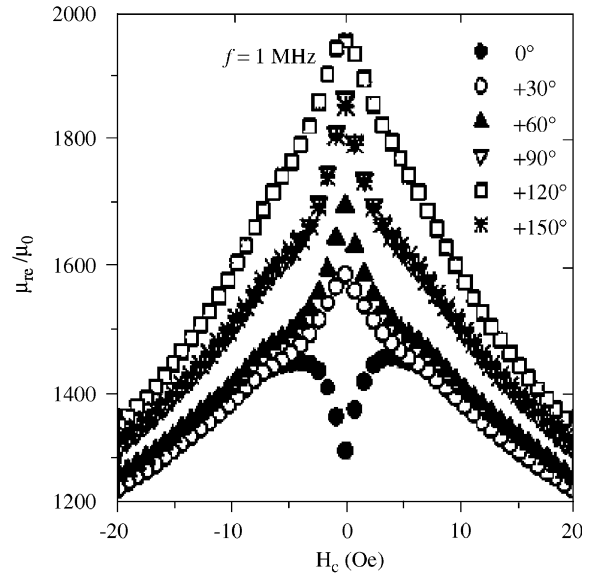


Fig. 6. MI plot of a CoFeBSi wire, as a function of the torsion angle. The length of the wire was 10 cm [15].

The possibility to combine low-frequency MI measurements (where the impedance response is associated essentially with transversal domain walls) with longitudinal measurements carried out by placing the sample in a coil driven by the AC field (where the impedance response depends mainly on longitudinal domain walls) can lead to a characterization of the domain wall arrangement on the sample. A low transverse permeability (with a high relaxation frequency) and a large longitudinal permeability (with a low relaxation frequency) can then be interpreted in terms of a domain wall system with long domain walls parallel to the ribbon axis, with small, transverse walls, strongly pinned to the external surface of the ribbon [25].

#### 5. Conclusions

Domain wall dynamics is a complex process; however, inductance spectroscopy and magnetoimpedance have been developed enough to become powerful tools as characterization methods for soft ferro- and ferrimagnetic materials.

## References

- [1] R. Valenzuela, *J. Alloys Compounds* 369 (2004) 40.
- [2] R. Valenzuela, *J. Magn. Magn. Mater.* 249 (2002) 300.
- [3] K.L. Garcia, R. Valenzuela, *J. Appl. Phys.* 87 (2000) 5257.
- [4] E.P. Harrison, G.L. Turney, H. Rowe, *Nature* 135 (1935) 961.
- [5] M. Vázquez, M. Knobel, M.L. Sánchez, R. Valenzuela, A. Zhukov, *Sensors Actuators A* 59 (1997) 20.
- [6] M. Knobel, M. Vázquez, L. Krauss, Giant magnetoimpedance, in: K.H.J. Buschow (Ed.), *Handbook of Magnetic Materials*, Elsevier Science, Amsterdam, 2003, p. 497.
- [7] K.R. Pirota, M.L. Sartorelli, M. Knobel, J. Gutiérrez, J.M. Barandiarán, *J. Magn. Magn. Mater.* 202 (1999) 431.
- [8] R.S. Beach, A.E. Berkowitz, *J. Appl. Phys.* 76 (1994) 6209.
- [9] H.Q. Guo, H. Kronmuller, T. Dragon, C. Chen, B.G. Shen, *J. Appl. Phys.* 84 (1998) 5673.
- [10] J.M. Barandiarán, A. Hernando, *J. Magn. Magn. Mater.* 268 (2004) 309.
- [11] M.T. González, K.L. García, R. Valenzuela, *J. Appl. Phys.* 85 (1999) 319.
- [12] L.P. Shen, T. Uchiyama, K. Mohri, E. Kita, K. Bushida, *IEEE Trans. Magn.* 33 (1997) 3355.
- [13] J.M. Blanco, A. Zhukov, J. Gonzalez, *J. Magn. Magn. Mater.* 196–197 (1999) 377.
- [14] M. Tejedor, B. Hernando, M.L. Sanchez, V.M. Prida, M. Vazquez, *J. Phys. D* 31 (1999) 3331.
- [15] I. Betancourt, R. Valenzuela, *Appl. Phys. Lett.* 83 (2003) 2022.
- [16] K.L. Garcia, R. Valenzuela, *IEEE Trans. Magn.* 34 (1998) 1162.
- [17] R. Valenzuela, M. Knobel, M. Vázquez, A. Hernando, *J. Appl. Phys.* 78 (1995) 5189.
- [18] J.R. McDonald, *Impedance Spectroscopy*, Wiley, New York, 1987 (Chapter 2).
- [19] M.I. Rosales, O. Ayala, R. Valenzuela, *IEEE Trans. Magn.* 37 (2001) 2373.
- [20] P. Quintana, E. Amano, R. Valenzuela, J.T.S. Irvine, *J. Appl. Phys.* 75 (1994) 6940.
- [21] M.K. Kazimierzczuk, G. Sancineta, G. Grandi, U. Reggiani, A. Massarini, *IEEE Trans. Magn.* 35 (1999) 4185.
- [22] E.M. Gyorgy, in: N.B. Hannay (Ed.), *Treatise in Solid State Chemistry: Defects in Solids*, vol. 2, Plenum Press, New York, 1975, p. 395.
- [23] M. Herrera, M.Sc. Thesis, National University of Mexico, 2004.
- [24] R. Valenzuela, J.T.S. Irvine, *J. Appl. Phys.* 72 (1992) 1486.
- [25] P. Garcia-Tello, J. González, R. Valenzuela, *J. Non-Cryst. Solids* 329 (2003) 144.